A Texture Analysis–Based Prediction Model for Lymph Node Metastasis in Stage IA Lung Adenocarcinoma

Yawei Gu, MD,* Yunlang She, MD,* Dong Xie, MD, PhD,* Chenyang Dai, MD, Yijiu Ren, MD, Ziwen Fan, MD, Huiyuan Zhu, MD, Xiwen Sun, MD, Huikang Xie, MD, Gening Jiang, MD, and Chang Chen, MD, PhD

Departments of Thoracic Surgery, Radiology, and Pathology, Shanghai Pulmonary Hospital, Tongji University School of Medicine, Shanghai, People's Republic of China

Background. **Some clinical N0 lung adenocarcinomas have been pathologically diagnosed as N1 or N2. To improve the preoperative diagnostic accuracy of lymph node disease, we developed a prediction model for lymph node metastasis in cT1 N0 M0 lung adenocarcinoma based on computed tomography texture analysis and clinical characteristics to estimate the probability of lymph node metastasis.**

Methods. **The records of 501 consecutive patients with cT1 N0 M0 lung adenocarcinoma who underwent computed tomography scan and pulmonary resection with systematic lymph nodes dissection or lymph nodes sampling were reviewed. Each nodule was manually segmented, and its computerized texture features were extracted. Multivariate logistic regression with fivefold validation was used to estimate independent predictors and build the prediction model. The prediction model was then externally validated. A nomogram was developed based on logistic regression results.**

Results. **Among 501 patients, 41 were diagnosed with positive lymph nodes (8.18%). Four independent predictors were identified: the skewness and 90th percentile of computed tomography number, nodule compactness, and carcinoembryonic antigen level. This model showed good calibration (Hosmer-Lemeshow test, $p = 0.337$), with an area under the curve of 0.883 (95% confidence interval, 0.842 to 0.924; $p < 0.001$). The area under the curve was 0.808 (95% confidence interval, 0.735 to 0.880) when validated with independent data.**

Conclusions. **A model based on computerized textures and carcinoembryonic antigen level can assess the lymph node status of patients with cT1 N0 M0 lung adenocarcinoma preoperatively, which could assist surgeons in making subsequent clinical decisions.**

(Ann Thorac Surg 2018;106:214–20)

With the introduction of computed tomography (CT) screening for lung cancer and the extensive use of low-dose CT, the detection rate of peripheral small lung cancer has increased [1]. Among patients with a peripheral tumor 3 cm or less in diameter, 5.6% to 20% with non-small cell lung cancer (NSCLC) were pathologically diagnosed as N1 or N2 [2–4], and many of them were clinically diagnosed as N0. Accurate staging of lymph nodes (LNs) is significant in NSCLC because it can influence the choice of optimal therapy and patients' prognosis.

At present, positron emission tomography (PET)–CT remains the best radiologic examination for assessing LN status. For highly suspicious involved LNs on PET-CT, further examinations, such as biopsy under mediastinoscopy or endobronchial ultrasound-guided transbronchial needle aspiration, are used for diagnosis. In China, however, PET-CT is not a common examination for early-stage tumors (≤3 cm) with no enlarged LNs on CT imaging due to its economic burden for patients. Furthermore, because patients would benefit little from invasive examinations without imaging evidence of LN involvement, these examinations can be omitted. Therefore, improving the diagnostic ability of CT imaging in assessing LN metastasis in patients with early-stage NSCLC is an urgent necessity, especially lung adenocarcinoma, because adenocarcinoma is confirmed to have a higher risk of LN invasiveness [5, 6].

Multiple published models have used primary tumor-specific factors on preoperative CT imaging to assess LN metastasis in patients with early-stage NSCLC with a

Accepted for publication Feb 12, 2018.

*Drs Gu, She, and Xie contributed equally to this work.

Address correspondence to Dr Chen, Department of Thoracic Surgery, Shanghai Pulmonary Hospital, Tongji University School of Medicine, 507 Zhengmin Rd, Shanghai 200443, China; email: chenthoracic@163.com.

The Supplemental Material can be viewed in the online version of this article [https://doi.org/10.1016/j.athoracsur.2018.02.026] on http://www.annalsthoracicsurgery.org.

0003-4975/$36.00
https://doi.org/10.1016/j.athoracsur.2018.02.026

clinically negative mediastinum [4, 7, 8]. However, these tumor-specific factors were usually obtained through visual assessment, in which individual error and interobserver error are inevitable.

CT texture analysis is a quantitative analysis tool that can obtain more detailed and quantitative data on the region of interest than visual assessment [9]. It can also transform the original data into derived features through variant mathematical transformations. CT texture analysis has been used to improve the accuracy in differentiating preinvasive pulmonary nodules from invasive nodules [10, 11] or premalignant pulmonary lesions from malignant lesions [12]. In this study, we sought to determine the most valuable CT texture features and clinical characteristics to develop a prediction model for LN metastasis in cT1 N0 M0 lung adenocarcinoma.

Patients and Methods

Ethical approval for this retrospective analysis was obtained from Shanghai Pulmonary Hospital, and the requirement for informed consent was waived.

Patients

The medical records of 811 patients with lung adenocarcinoma who underwent surgical resection at the Department of Thoracic Surgery, Shanghai Pulmonary Hospital, Tongji University, between January 2015 and December 2015 were retrospectively reviewed. Patients were included in our study if they had a solitary pulmonary nodule in clinical stage T1a based on CT imaging, no enlarged LNs were found, and they underwent lobectomy or sublobectomy with systematic LN dissection. Patients were excluded if they received neoadjuvant chemotherapy or radiotherapy before the operation, they had a history of malignant tumor, they underwent contrast-enhanced chest CT, or their CT images were not available. Patients who underwent an enhanced-contrast chest CT scan were excluded because the contrast agent might have an influence on the imaging features of nodules.

Clinical characteristics, including age, sex, smoking history, and carcinoembryonic antigen (CEA) level, were derived from medical records. Laboratory analysis of CEA was done by routine blood tests within 1 week before the operation. The CEA level threshold value was 5 ng/mL, according to the normal range used at our institution.

Between January 2015 and June 2015, 501 of the 811 patients were enrolled into the model-development cohort (group A), which was analyzed to build the prediction model. The remaining 310 patients between July 2015 and December 2015 were enrolled into group B for model validation.

Preoperative Investigations

All patients underwent a chest CT scan at our hospital before the operation. Other preoperative examinations included electrocardiography, lung function testing, brain magnetic resonance imaging or CT, bone scan, and abdominal CT or ultrasonography. None of the patients underwent preoperative biopsy.

CT Examinations and Computerized Texture Analysis

All patients underwent chest CT scan at Shanghai Pulmonary Hospital. The images were reconstructed using a medium-sharp reconstruction algorithm with a thickness of 1 to 1.25 mm. All chest CT scans were reviewed as lung window images (window width, 1,200 Hounsfield units [HU]; window level, −500 HU) and mediastinal window images (window width, 450 HU; window level, 50 HU).

The CT images were output and stored as Digital Imaging and Communications in Medicine images (National Electrical Manufacturers Association, Rosslyn, VA). Segmentation was performed manually by a radiologist (H.Z.) using an in-house software program (Medical Imaging Solution for Segmentation and Texture Analysis) and confirmed by another radiologist (X.S.) with more experience. Regions of interest were delineated freehand along the boundary of each nodule on every section in the CT images. Texture features were extracted from voxel data and calculated automatically. The features consisted of three groups: (1) first-order statistics based on a histogram of voxel intensify, including (*a*) mean, (*b*) SD, (*c*) skewness, (*d*) kurtosis, (*e*) entropy, (*f*) homogeneity, and (*g*) percentile (10th percentile and 90th percentile); (2) shape and size-based features, including (*a*) volume, (*b*) mass, (*c*) effective diameter, (*d*) surface area, (*e*) sphericity, (*f*) compactness, and (*g*) roundness; and (3) second-order texture features derived from gray-level co-occurrence matrix, including (*a*) inverse difference moment and (*b*) contrast.

Surgical Procedures and Pathologic Diagnosis

All patients underwent lobectomy or sublobectomy with systematic LN dissection or sampling. A wedge of the primary tumor was sent for frozen section before patients were considered for nodal dissection during a lobectomy for clinical stage I adenocarcinoma. Systematic LN dissection was performed in the same manner in all patients, and the minimal number of dissected LNs was 6. According to the European Society of Thoracic Surgeons guidelines [13], at least 3 mediastinal LN stations and a subcarinal station must be included. The hilar and intrapulmonary LNs were also excised. Pathologic LN stage was classified according to the lung cancer section of the TNM Classification of Malignant Tumours (Seventh Edition) [14].

Statistical Analysis

Clinical characteristics were analyzed between LN-positive and LN-negative groups by using the Fisher exact test or the χ^2 test for nominal categoric variables and the independent *t* test or Mann-Whitney *U* test for continuous variables. The univariable association between texture features and LN status was also analyzed by using the independent sample *t* test.

We randomly divided 501 patients in group A into five folds of approximately equal size. Four folds were the training cohort, and the remaining fold was the validation

cohort. This training-test procedure was repeated five times until all five folds were tested. In the training the cohort, we chose the variables with statistical significance ($p < 0.05$) in univariate analysis as input variables for binary logistic regression analysis. A backward stepwise selection mode (likelihood ratio) was used, with iterative entry of variables based on test results ($p < 0.05$). The removal of variables was based on likelihood ratio statistics with a probability of 0.10. Five logistic regression submodels were constructed. Variables with high frequency in the five submodels were used as input variables in binary logistic regression analysis using a forward stepwise mode (likelihood ratio) to build the final logistic regression model based on all data of group A [15].

To make the model more practicable, we convert the 90th percentile of the voxel histogram to integer units, with an increment of 100 HU as 1 unit, ranging from –7 to 2. The Hosmer-Lemeshow goodness-of-fit test ($p > 0.05$) was used to evaluate the model's fit. We then calibrated the model by dividing the sample into five equal groups based on the predicted probability of LN metastasis and plotting the median probability of each group vs the observed frequency. The area under the curve was used to assess the accuracy of the model. A nomogram based on the logistic regression model was also plotted. All analyses were performed by using SPSS Statistics 22.0 software (IBM, Armonk, NY) and R 3.4.0 software (The R Foundation for Statistical Computing, Vienna, Austria).

Results

There were 501 patients included in group A to develop our prediction model, and 41 (8.18%) were diagnosed with positive LNs. No significant differences were found in clinical characteristics between the LN-positive group and the LN-negative group, except in CEA level and tumor location (central vs peripheral; Table 1). The tumors with positive LN were more likely to be centrally located than peripherally located (9.76% vs 3.26%; $p < 0.05$). Patients with positive LNs also tended to have higher serum CEA level (CEA >5 ng/mL, 34.14% vs 6.10%; $p < 0.001$).

In univariate analysis of texture features, the 10th percentile, 90th percentile, SD, homogeneity, and mean of the voxel intensity histogram; effective diameter, volume, and surface area of the lesion; and the inverse difference moment were significantly higher in LN-positive lesions than in LN-negative lesions ($p < 0.05$; Table 2). The skewness and kurtosis of the voxel histogram, and the roundness, compactness, and sphericity of the nodule were significantly lower in LN-positive lesions than in LN-negative lesions ($p < 0.05$; Table 2).

Five top stable variables were determined in five submodels and were included in multivariate logistic regression (Table 3). Binary logistic regression analysis showed that smaller skewness and higher 90th percentile of voxels histogram, lower nodule compactness, and higher CEA level were independent predictors (Table 4). From these analytic results we built a formula and a nomogram to assess the probability of LN metastasis. The formula is expressed as follows: $p = ex/(1 + ex)$, $X = -3.4605 + 1.513 \times$ CEA level $-1.469 \times$ skewness $+ 0.768 \times$ 90th percentile $- 4.822 \times$ compactness (formula elucidation in the Supplemental Material).

Table 1. Clinical and Demographic Features of Lymph Node–Positive and Lymph–Node Negative Patients

Characteristics	Lymph Node Metastasis		p Value[a]
	Negative (n = 460) No.	Positive (n = 41) No.	
Age, years			
≤60	246	26	0.221
>60	214	15	
Sex			
Male	194	23	0.085
Female	266	18	
Smoking history			
Never	286	24	0.646
Current or former	174	17	
CEA, ng/mL			
≤5	432	27	<0.001[b]
>5	28	14	
Tumor location			
Central	15	4	0.037[b]
Peripheral	445	37	
Right lobe			
Upper	152	16	0.323
Middle	43	2	
Lower	72	6	
Left lobe			
Upper lobe	113	6	
Lower lobe	80	11	

[a] The p value is derived from the univariable association analysis between each of the variables and lymph node status. [b] Statistically significant ($p < 0.05$).

CEA = carcinoembryonic antigen; No. = number.

The Hosmer-Lemeshow goodness-of-fit test was not statistically significant ($p = 0.337$), indicating a high concordance between predicted likelihood and observed frequency. The calibration curve (Fig 1) of the model was satisfied. The area under the curve was 0.883 (95% CI, 0.842 to 0.924; $p < 0.001$; Fig 2), which showed reasonable accuracy. The nomogram is presented in Figure 3. External validation of the prediction model was performed using group B. The accuracy of our prediction model was good, with an area under the curve of 0.808 (95% CI, 0.735 to 0.880; Fig 4).

Comment

Even in the same T stage, the invasiveness of small pulmonary nodules varies substantially. The risk of LN involvement was correlated with the characteristics of a nodule [4–6]. Mere assessment based on the size of the lesion might lead to misdiagnosis of LN disease, especially in early-stage lung cancer, in which LNs might be

Table 2. Comparison of Texture Features Between Lesions With and Without Lymph Node Metastasis

Features[a]	Lymph Node Metastasis		*p* Value[b]
	Negative n = 460	Positive n = 41	
First order statistics			
Mean CT attenuation, HU	–471.62 ± 164.09	–267.78 ± 119.30	<0.001[c]
SD, HU	217.16 ± 71.44	277.94 ± 43.87	<0.001[c]
Skewness	0.29 ± 0.64	–0.47 ± 0.58	<0.001[c]
Kurtosis	2.70 ± 1.42	2.19 ± 0.91	0.002[c]
Entropy	4.75 ± 0.40	4.85 ± 0.31	0.059
CT attenuation, HU			
10th percentile	–747.73 ± 97.19	–671.36 ± 127.51	0.001[c]
90th percentile	–182.81 ± 217.52	41.77 ± 27.53	<0.001[c]
Shape and size statistics			
Effective diameter, mm	24.44 ± 9.67	31.16 ± 6.67	<0.001[c]
Volume, mm^3	4570.31 ± 5152.18	7994.40 ± 4253.19	<0.001[c]
Surface area, mm	2086.51 ± 1828.18	3251.47 ± 1425.76	<0.001[c]
Sphericity	0.634 ± 0.097	0.597 ± 0.067	0.002[c]
Compactness	0.273 ± 0.120	0.221 ± 0.075	<0.001[c]
Roundness	0.689 ± 0.104	0.653 ± 0.074	0.006[c]
Second-order texture features			
Homogeneity	0.381 ± 0.051	0.408 ± 0.043	0.001[c]
Inverse difference moment	0.302 ± 0.060	0.339 ± 0.051	<0.001[c]
Contrast	24.29 ± 11.24	29.384 ± 7.173	<0.001[c]

[a] Data are shown as mean values ± SD. [b] The *p* values are derived from the univariable association analysis between each of the variable and lymph node status. [c] Statistically significant ($p < 0.05$.)

CT = computed tomography; HU = Hounsfield unit.

underestimated without any enlargement of LNs on CT imaging. Although PET-CT has been an effective noninvasive method in preoperative LN staging, the accuracy decreased when a LN was less than 10 mm [16, 17].

Beside information derived from LNs, characteristics of the primary tumor and clinical data of the patients are also useful in LN staging. Previous studies developed several prediction models for N2 disease in NSCLC [8, 18, 19]. In these models, younger age, larger tumor size, central tumor location, and adenocarcinoma were independent predictors. However, these studies put little emphasis on the features of tumors, whereas more and more studies have confirmed that manifestations of a nodule on CT imaging are related to its characteristics [20–22]. Computerized texture analysis is an approach that makes the best use of CT information from a more precise and objective perspective.

By using logistic regression and cross-validation, we built a prediction model based on primary tumors' computerized texture features and patients' clinical data. We included the top five variables in the five submodels (from each training fold) into the logistic regression. The prediction model showed good calibration and accuracy and was externally validated by an independent data set. The predictors in our model were also identified in other studies. Ye and colleagues [4] and Koike and colleagues [23] found that patients with an elevated preoperative

Table 3. Frequency of Computed Tomography Features in Five Submodels

Features	Submodel				
	1	2	3	4	5
CEA level	✓	✓	✓	✓	✓
90th percentile	✓	✓	✓	✓	✓
Compactness	✓	✓	✓	✓	
Skewness	✓			✓	✓
Roundness		✓	✓	✓	
10th percentile			✓		✓
IDM		✓	✓		✓
SD			✓		✓
Kurtosis					✓
Tumor location		✓			

CEA = carcinoembryonic antigen; IDM = inverse difference moment.

Table 4. Results of Multivariate Logistic Regression Analysis

Variables	Odds Ratio	95% CI	*p* Value
CEA level	4.541	1.870–11.028	0.001[a]
Skewness	0.230	0.102–0.519	<0.001[a]
90th percentile[b]	2.156	1.029–4.518	0.042[a]
Compactness	0.010	0.000–0.788	0.039[a]

[a] Statistically significant ($p < 0.05$.) [b] 100 Hounsfield units as 1 unit.

CEA = carcinoembryonic antigen; CI = confidence interval.

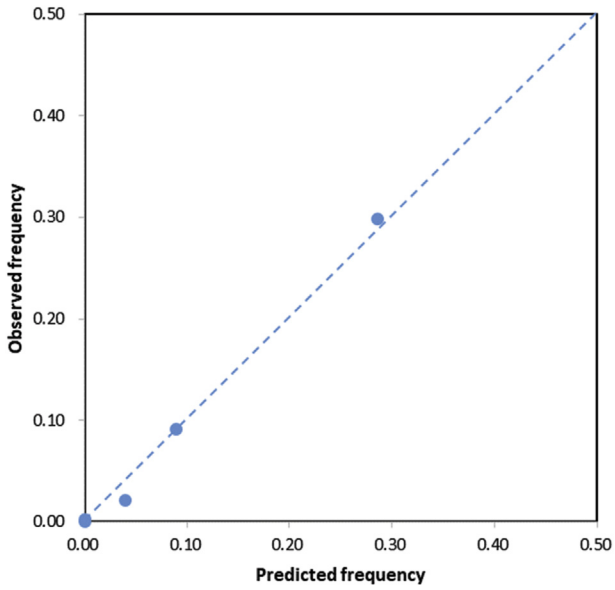

Fig 1. The calibration curve for the clinical prediction model. The curve showed that the observed frequency of lymph node metastasis was similar to the predicted probability for patients in each quintile: 1 (0.000, 0.000), 2 (0.000, 0.003), 3 (0.040, 0.022), 4 (0.089, 0.091), and 5 (0.286, 0.298).

serum CEA level were more likely to have LN involvement. The 90th percentile and skewness of the voxel intensity histogram were both descriptors of the voxel distribution of a nodule; usually, a more solid nodule would have higher 90th percentile and smaller skewness.

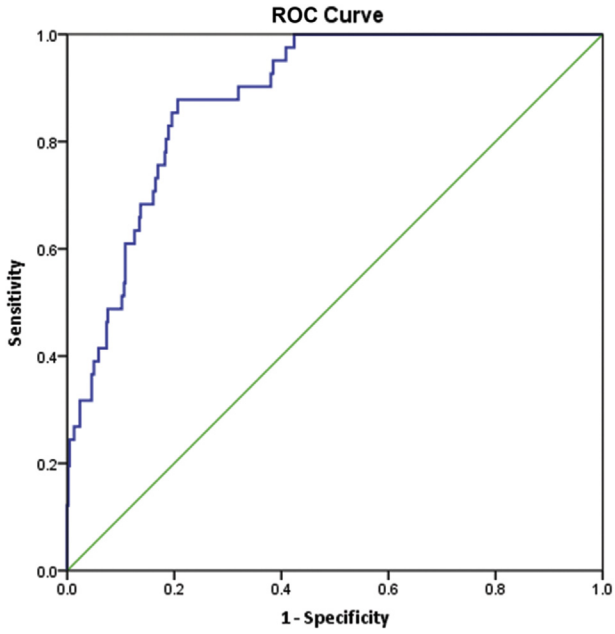

Fig 2. The receiver operating characteristic curve (ROC) for the prediction of lymph node metastasis in group A by using a logistic regression model. The area under the curve is 0.883 (95% confidence interval, 0.842 to 0.924; $p < 0.01$).

In our study, the voxel intensity histogram of LN-positive nodules had higher 90th percentile but a smaller skewness compared with LN-negative nodules. In a study by Chae and colleagues [10], for the partly solid nodules, invasive pulmonary adenocarcinomas had a higher 90th percentile of voxel intensity histogram with smaller skewness. A LN-positive nodule also has lower compactness. This feature (formula of compactness in the Supplemental Material) reflects the relationship between volume and surface area of the nodules. Our data showed that LN-positive nodules had a larger volume with bigger surface area but lower compactness compared with LN-negative nodules.

We also built a nomogram, with which pretest probability can be obtained visually. If the serum CEA level was higher than 5 ng/mL (value as 2), the 90th percentile was 100 (value as 1), skewness was –0.5, and compactness was 0.25, the probability of LN metastasis for the patient was 46.57% based on the formula and approximately 45% (200 points) according to the nomogram. Further diagnostic examinations, such as PET-CT, mediastinoscopy, or endobronchial ultrasound-guided transbronchial needle aspiration would be essential for this patient because the probability was higher than the cutoff value of 11.40% from the receiver operating characteristic curve. If the probability were lower than 11.40%, the possibility of LNs metastasis might be low, and invasive examinations would offer little benefit. It is important to note that the result of our prediction model can only be used as a reference for clinicians in decision making before further invasive examinations. Confirmative conclusions cannot be drawn from this result.

To our knowledge, this is the first study in differentiating LN-positive early-stage lung adenocarcinoma from LN-negative adenocarcinoma based on texture analysis of the primary pulmonary nodules. Some studies have focused on the CT textures of LNs in patients with lung cancer, discriminating the benign from the malignant ones [24, 25], and the size of the target LNs was usually larger than 1 cm [25]. However, enlarged LNs are rarely observed for patients with early-stage lung cancer, so contrast-enhanced CT or PET-CT would offer limited benefit. We therefore had to put more emphasis on the features of primary pulmonary nodules on CT.

Coroller and colleagues [26] applied texture analysis of both primary tumor and LNs in predicting pathologic response. Huang and colleagues [27] used a radiomic nomogram, which was also based on CT texture analysis of the primary tumor, to predict LN metastasis in patients with colorectal cancer. These studies indicated that texture analysis of the primary tumor was reasonable. Information obtained from the nodules would tell us about the growth pattern and the invasiveness of the tumors, including invasion of LNs. More reliable results might be found if we combined CT texture features of both primary tumors and LNs, but the feasibility and efficiency of this method are unknown.

Our study also has some limitations. Although we built a prediction model through cross-validation, patient selection bias was inevitable because of the retrospective

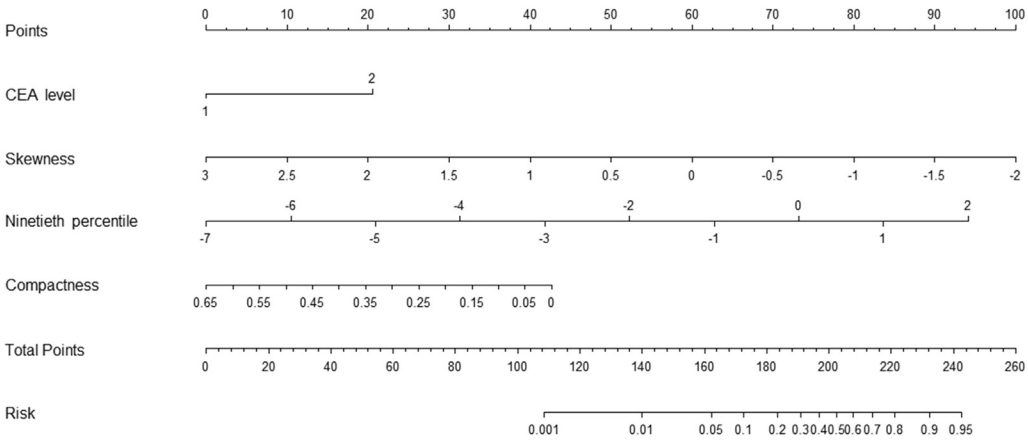

Fig 3. Nomogram for predicting the probability of lymph node (LN) metastasis. To obtain the predicted probability, locate the patient values at each axis, and draw a vertical line to the "Points" axis to determine the number of points attributed to each variable value, determine total number of points for all variables, and locate the sum on the "Total Points" line to assess the individual probability of LN metastasis, Carcinoembryonic antigen (CEA) level is the CEA level with 5 ng/mL as cutoff value.

collection of data, which might lead to bias in the selection of texture features. Prospective multiinstitutional studies are required to further validate the model. In addition, we did not compare the difference between lung adenocarcinoma and other lung cancers, which also may limit its application in clinical practice.

In conclusion, we developed a prediction model based on CT texture features and CEA level to estimate the probability of LN metastasis in patients with clinical stage IA lung adenocarcinoma. The predicted results can partially differentiate nodules at high risk of LN metastasis from those at low risk, which may be helpful in subsequent clinical treatment.

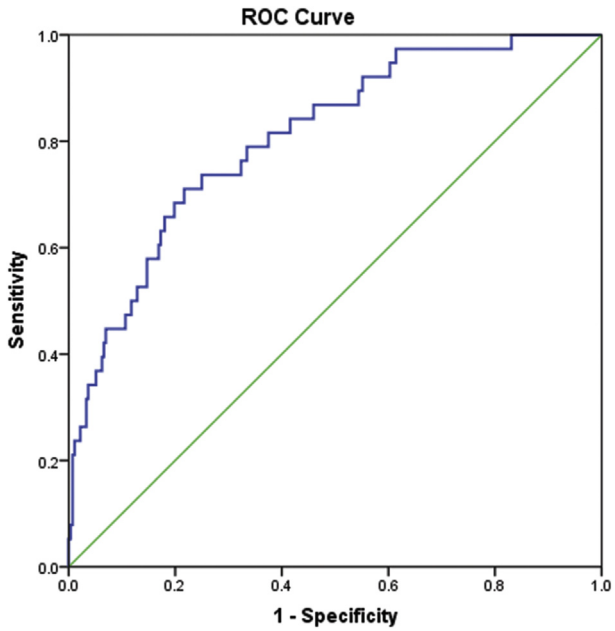

Fig 4. The receiver operating characteristic (ROC) curve for the prediction in group B. The area under the curve is 0.808 (95% confidence interval, 0.735 to 0.880; $p < 0.01$).

This work was supported by the projects from Shanghai Hospital Development Center (16CR3116B).

References

1. Aberle DR, Adams AM, Berg CD, et al. Reduced lung-cancer mortality with low-dose computed tomographic screening. N Engl J Med 2011;365:395–409.
2. Ishida T, Yano T, Maeda K, Kaneko S, Tateishi M, Sugimachi K. Strategy for lymphadenectomy in lung cancer three centimeters or less in diameter. Ann Thorac Surg 1990;50:708–13.
3. Takizawa T, Terashima M, Koike T, et al. Lymph node metastasis in small peripheral adenocarcinoma of the lung. J Thorac Cardiovasc Surg 1998;116:276–80.
4. Ye B, Cheng M, Li W, et al. Predictive factors for lymph node metastasis in clinical stage Ia lung adenocarcinoma. Ann Thorac Surg 2014;98:217–23.
5. Suzuki K, Nagai K, Yoshida J, Nishimura M, Takahashi K, Nishiwaki Y. Clinical predictors of N2 disease in the setting of a negative computed tomographic scan in patients with lung cancer. J Thorac Cardiovasc Surg 1999;117:593–8.
6. Kanzaki R, Higashiyama M, Fujiwara A, et al. Occult mediastinal lymph node metastasis in NSCLC patients diagnosed as clinical N0-1 by preoperative integrated FDG-PET/CT and CT: risk factors, pattern, and histopathological study. Lung Cancer 2011;71:333–7.
7. Seok Y, Yang HC, Kim TJ, et al. Frequency of lymph node metastasis according to the size of tumors in resected pulmonary adenocarcinoma with a size of 30 mm or smaller. J Thorac Oncol 2014;9:818–24.
8. Zhang Y, Sun Y, Xiang J, Zhang Y, Hu H, Chen H. A prediction model for N2 disease in T1 non-small cell lung cancer. J Thorac Cardiovasc Surg 2012;144:1360–4.
9. Aerts HJ, Velazquez ER, Leijenaar RT, et al. Decoding tumour phenotype by noninvasive imaging using a quantitative radiomics approach. Nat Commun 2014;5:4006.
10. Chae HD, Park CM, Park SJ, Lee SM, Kim KG, Goo JM. Computerized texture analysis of persistent part-solid ground-glass nodules: differentiation of preinvasive lesions from invasive pulmonary adenocarcinomas. Radiology 2014;273:285–93.
11. Hwang IP, Park CM, Park SJ, et al. Persistent pure ground-glass nodules larger than 5 mm: differentiation of invasive pulmonary adenocarcinomas from preinvasive lesions or

minimally invasive adenocarcinomas using texture analysis. Invest Radiol 2015;50:798–804.
12. Ikeda K, Awai K, Mori T, Kawanaka K, Yamashita Y, Nomori H. Differential diagnosis of ground-glass opacity nodules: CT number analysis by three-dimensional computerized quantification. Chest 2007;132:984–90.
13. Lardinois D, De Leyn P, Van Schil P, et al. ESTS guidelines for intraoperative lymph node staging in non-small cell lung cancer. Eur J Cardiothorac Surg 2006;30:787–92.
14. Goldstraw P, Crowley J, Chansky K, et al. The IASLC lung cancer staging project: proposals for the revision of the TNM stage groupings in the forthcoming (seventh) edition of the TNM Classification of Malignant Tumours. J Thorac Oncol 2007;2:706–14.
15. Mosteller F, Tukey JW. Data analysis, including statistics. Reading, MA: Addison-Wesley; 1968.
16. Bille A, Pelosi E, Skanjeti A, et al. Preoperative intrathoracic lymph node staging in patients with non-small-cell lung cancer: accuracy of integrated positron emission tomography and computed tomography. Eur J Cardiothorac Surg 2009;36:440–5.
17. Nomori H, Watanabe K, Ohtsuka T, Naruke T, Suemasu K, Uno K. The size of metastatic foci and lymph nodes yielding false-negative and false-positive lymph node staging with positron emission tomography in patients with lung cancer. J Thorac Cardiovasc Surg 2004;127:1087–92.
18. Shafazand S, Gould MK. A clinical prediction rule to estimate the probability of mediastinal metastasis in patients with non-small cell lung cancer. J Thorac Oncol 2006;1:953–9.
19. Chen K, Yang F, Jiang G, Li J, Wang J. Development and validation of a clinical prediction model for N2 lymph node metastasis in non-small cell lung cancer. Ann Thorac Surg 2013;96:1761–8.
20. Shimada Y, Yoshida J, Hishida T, Nishimura M, Ishii G, Nagai K. Predictive factors of pathologically proven noninvasive tumor characteristics in T1aN0M0 peripheral non-small cell lung cancer. Chest 2012;141:1003–9.
21. Suzuki K, Koike T, Asakawa T, et al. A prospective radiological study of thin-section computed tomography to predict pathological noninvasiveness in peripheral clinical Ia lung cancer (Japan Clinical Oncology Group 0201). J Thorac Oncol 2011;6:751–6.
22. Lee SM, Park CM, Goo JM, Lee HJ, Wi JY, Kang CH. Invasive pulmonary adenocarcinomas versus preinvasive lesions appearing as ground-glass nodules: differentiation by using CT features. Radiology 2013;268:265–73.
23. Koike T, Koike T, Yamato Y, Yoshiya K, Toyabe S. Predictive risk factors for mediastinal lymph node metastasis in clinical stage Ia non-small-cell lung cancer patients. J Thorac Oncol 2012;7:1246–51.
24. Bayanati H, Thornhill RE, Souza CA, et al. Quantitative CT texture and shape analysis: can it differentiate benign and malignant mediastinal lymph nodes in patients with primary lung cancer? Eur Radiol 2015;25:480–7.
25. Andersen MB, Harders SW, Ganeshan B, Thygesen J, Torp Madsen HH, Rasmussen F. CT texture analysis can help differentiate between malignant and benign lymph nodes in the mediastinum in patients suspected for lung cancer. Acta Radiol 2016;57:669–76.
26. Coroller TP, Agrawal V, Huynh E, et al. Radiomic-based pathological response prediction from primary tumors and lymph nodes in NSCLC. J Thorac Oncol 2017;12:467–76.
27. Huang YQ, Liang CH, He L, et al. Development and validation of a radiomics nomogram for preoperative prediction of lymph node metastasis in colorectal cancer. J Clin Oncol 2016;34:2157–64.